

In-silico discovery of a high-affinity aptamer for CA125 enables rapid detection via lateral flow assay

Vandana Tandasi¹, and Sudha Srivastava^{1,2*}

¹Department of Biotechnology, Jaypee Institute of Information Technology, A-10, Sector-62, NOIDA, INDIA.

²Department of Chemistry, Jaypee Institute of Information Technology, A-10, Sector-62, NOIDA, INDIA.

*Corresponding author: sudha.srivastava@mail.jiit.ac.in

ABSTRACT

Rapid and accessible detection of ovarian cancer biomarkers remains a major challenge for effective point-of-care diagnostics. Of these, CA125 is majorly used for disease diagnostics. However, current detection methods are constrained by cost, complexity, and limited portability. In the present study, we proposed an integrated methodology by combining bioinformatics-driven aptamer discovery with lateral flow assay (LFA) development. A huge library of ssDNA ($\sim 4.1 \times 10^6$ sequences) was thoroughly screened by using computational tools to identify high-affinity aptamer candidates, which resulted in the selection of a novel aptamer (P1) with superior predicted binding performance relative to existing sequences. The selected aptamer was subjected to conjugation with gold nanoparticles and incorporated into a Lateral Flow Assay platform for rapid detection. The developed assay showed clear and reproducible visual detection of CA125 antigen at 10 ng/mL. This study establishes a systematic pipeline which links *in-silico* aptamer design with practical diagnostic implementation, which offers a scalable and cost-effective approach for next-generation point-of-care cancer biosensors.

Keywords: CA125, Aptamer, In silico screening, Bioinformatics, Lateral Flow Assay, Gold nanoparticles (AuNPs), Point-of-care diagnostics, Ovarian cancer biomarker

1. INTRODUCTION

Cancer still remains one of the leading causes of deaths over the globe, with ovarian cancer being among the most lethal gynecological cancer because of its asymptomatic presentation at early stages and late diagnosis [1]. Early detection significantly improves patient survival. However, the lack of rapid, accessible, and reliable diagnostic tools continues to be a major challenge. Among multiple biomarkers, CA125 is widely used for the monitoring and management of ovarian cancer. Despite its widespread clinical use, CA125 exhibits limited specificity, as elevated levels are also observed in several non-cancerous conditions, thereby reducing its diagnostic accuracy [2], [3].

The conventional detection methods for CA125, e.g., enzyme-linked immunosorbent assays (ELISA), chemiluminescence assays, and imaging-based diagnostics, are often time-taking, costly, and require complex laboratory infrastructure [4], [5]. As a result, these techniques are not suited for application in resource-limited settings and restrict their use for rapid, point-of-care (POC) testing. As shown in recent studies, there is a raised demand for POC diagnostic tools that enable timely disease detection and monitoring while minimizing the burden on healthcare systems [6].

In this regard, Lateral Flow Assay (LFA) has emerged as a promising platform for POC diagnostics due to its simplicity, rapid response, low cost, and ease of use. LFA-based systems have been widely adopted in clinical and settings. However, their application in cancer biomarker detection remains limited by challenges such as insufficient sensitivity, poor quantitative capability, and dependence on antibody-based recognition elements [7], [8], [9], [3]. Recent advancements have focused on improving LFA performance through the use of nanomaterials, signal amplification strategies, and multiplex detection approaches, including the use of nanozymes and luminescent nanoparticles to enhance analytical sensitivity [6], [10].

The biorecognition element is a critical component of LFA systems, which has traditionally relied on antibodies. Although antibodies offer higher specificity, they have certain limitations for instances, high production cost, batch-to-batch variations, limited stability under harsh conditions, and ethical concerns associated with animal use [11], [9], [12], [10]. The investigation of alternate recognition components, like aptamers, has been prompted by these constraints. Short single-stranded nucleic acids known as aptamers have the capacity to bind targets with high affinity and specificity while also providing benefits including chemical stability, simplicity in production, and repeatability. The promise of aptamers in CA125 detection has been shown in a number of studies, including their incorporation into lateral flow and nanozyme-based systems for quick diagnosis [12], [10].

Despite these developments, classic SELEX-based methods have been used to identify the majority of reported aptamers for CA125. These methods are time-consuming, labor-intensive, and frequently provide a huge pool of candidate sequences that require considerable experimental validation. To enhance aptamer selection, recent attempts have tried to incorporate computational methods with SELEX. However, there is still a lack of research on entirely bioinformatics-driven pathways for aptamer discovery [13], [14], [15]. Furthermore, while several LFA systems for CA125 detection have been reported, many rely on complex signal amplification strategies or multiplexed formats, which may compromise simplicity and cost-effectiveness required for point-of-care applications [16], [17].

Thus, a straightforward, effective, and scalable method that combines quick aptamer discovery with useful diagnostic implementation is desperately needed. In this study, we address this gap by developing a novel aptamer for CA125 using a comprehensive *in silico* screening pipeline, followed by its integration into a gold nanoparticle-based lateral flow assay. In contrast to traditional methods, the suggested technique makes use of bioinformatics tools for large-scale sequence screening, structural assessment, and interaction analysis, allowing for the more effective discovery of high-affinity aptamer candidates.

The selected aptamer was experimentally validated and employed in the development of an aptamer–AuNP-based LFA for the rapid detection of CA125. The assay was evaluated for its ability to generate a visible signal at clinically relevant concentrations, demonstrating its potential as a proof-of-concept platform for point-of-care diagnostics. This work highlights the feasibility of integrating computational aptamer design with LFA technology and provides a foundation for the development of next-generation diagnostic tools for cancer biomarker detection.

2. Methodology

2.1 *In Silico* Design and Screening of Aptamer for CA125

The high-affinity aptamers specific to CA125 were designed and screened by using a systematic *in-silico* screening pipeline which aimed at identifying candidates with optimal structural stability and binding specificity. In the first stage, a random single-stranded DNA (ssDNA) library comprised of oligonucleotide sequences of 30–45 nucleotides in length was generated using FaBox [18].

This was developed to maintain a suitable length range for effective folding and target interaction while assuring adequate sequence diversity. The redundant sequences with low-complexity were excluded to enhance the quality of the initial pool. The generated sequences were further subjected to preliminary screening using the PPAI webserver [19], which evaluates aptamer likelihood based on intrinsic sequence and structural properties. Each sequence was assigned an aptamer probability score derived from multiple parameters, including nucleotide composition bias, GC content (maintained within an optimal range of 40–60% to balance structural stability and flexibility), and predicted secondary structure features.

Sequences that can form stable conformations, like stem-loop structures and G-quadruplex-like motifs, which are known to increase target binding affinity, were found using structural folding analysis. Minimum free energy (MFE) computations were used to evaluate the thermodynamic stability of various conformations which means more stable structures were indicated by lower MFE values. Sequences with poorly defined secondary structures or unfavorable thermodynamic profiles were not included in the analysis. Following preliminary filtration, the shortlisted candidates were subjected to detailed interaction analysis with CA125 using the protein-aptamer interaction module integrated within the PPAI platform.

2.2 Molecular Docking and Candidate Refinement

Further refinement of the shortlisted aptamer candidates was carried out through molecular docking analysis using HDOCK and pyDock. The three-dimensional structures of the selected aptamers were generated and used as ligands, while the target structure of CA125 was employed as the receptor for docking simulations.

Docking was performed to evaluate the binding interactions between each aptamer candidate and the target protein. The resulting complexes were ranked based on binding energy scores and interaction parameters obtained from both docking platforms. From each tool, the top 10 aptamer candidates exhibiting the most favorable binding energies were selected.

To ensure robustness and consistency in prediction, candidates that were commonly ranked among the top-performing sequences across both HDOCK [20] and pyDock [21] analyses were identified and shortlisted for further evaluation.

To assess the specificity of the selected aptamer candidates, off-target binding analysis was conducted against a panel of 37 cancer-associated biomarkers. The three-dimensional structures of these proteins were retrieved from the Protein Data Bank (PDB).

Each shortlisted aptamer was subjected to docking simulations against these off-target proteins using the same computational pipeline. Binding interactions were analyzed and compared with those obtained for CA125.

The interaction assessment was based on multiple parameters, including predicted binding free energy (ΔG_{bind}), hydrogen bonding interactions, electrostatic complementarity, and shape complementarity indices.

Based on comprehensive evaluation of docking scores, thermodynamic stability, and structural compatibility with the target epitope, the highest-scoring aptamer candidate, designated as P1, was selected as a putative high-affinity binder. This candidate was subsequently carried forward for experimental validation and integration into a lateral flow assay platform to assess its practical diagnostic applicability.

2.3 Synthesis of Gold Nanoparticles (AuNPs) for LFA development

Gold nanoparticles (AuNPs) were synthesized using the classical citrate reduction method [22], which enables the formation of monodispersed colloidal nanoparticles with controlled size distribution which was visually confirmed by a characteristic color transition from pale yellow to deep wine red within approximately 10 minutes.

2.4 Characterization of AuNPs

The synthesized AuNPs were characterized using UV–visible spectroscopy to confirm nanoparticle formation and optical properties. Absorption spectra were recorded over a wavelength range of 190–1100 nm. A distinct surface plasmon resonance (SPR) peak was observed at approximately 521 nm, which is characteristic of spherical gold nanoparticles and indicative of successful synthesis.

2.5 Preparation of Biotinylated Aptamer–AuNP Conjugates

A 5'-biotinylated DNA aptamer (P1), designed against CA125, was employed for nanoparticle functionalization. Conjugation was achieved through non-covalent adsorption of the aptamer onto the AuNP surface, driven by electrostatic interactions and the inherent affinity of nucleobases toward gold surfaces.

Briefly, AuNPs were incubated with the aptamer at a final concentration of 5 μ M under gentle mixing conditions to facilitate uniform surface adsorption. The incubation was carried out under controlled conditions to ensure optimal surface coverage without inducing nanoparticle aggregation.

Following incubation, the conjugated nanoparticles were centrifuged at 7000 rpm for 15 minutes to remove excess unbound aptamer. The supernatant was carefully discarded, and the resulting pellet was resuspended in 100 μ L of resuspension buffer to obtain stabilized aptamer–AuNP conjugates.

The presence of the biotin moiety at the 5' end of the aptamer was retained to enable potential downstream applications such as affinity-based capture or controlled orientation, without interfering with nanoparticle binding.

2.6 Fabrication of Lateral Flow Assay (LFA) Strips

The lateral flow assay strips were constructed using a standard multi-component assembly comprising a sample pad, conjugate pad, nitrocellulose membrane, and absorbent pad.

The test line was prepared by immobilizing anti-CA125 antibody (0.40 μ g/cm) onto the nitrocellulose membrane using carbonate–bicarbonate buffer (pH 9.5). Dispensing was carried out using a BioDot dispensing system to ensure uniform and reproducible deposition.

The control line was prepared by immobilizing streptavidin onto the nitrocellulose membrane at an optimized concentration. The use of streptavidin enables specific capture of the 5'-biotinylated aptamer–AuNP conjugates via strong biotin–streptavidin interaction, thereby serving as an internal procedural control to confirm proper sample flow and conjugate functionality.

The membrane was incubated overnight at room temperature to ensure stable adsorption of both test and control line reagents.

The conjugate pad was loaded with 50 μ L of the prepared biotinylated aptamer–AuNP conjugates and dried overnight under ambient conditions. Subsequently, the sample pad, conjugate pad, nitrocellulose membrane, and absorbent pad were assembled sequentially onto an adhesive backing card with appropriate overlaps to facilitate uninterrupted capillary-driven flow.

The assembled sheets were then cut into individual strips of uniform dimensions for further evaluation.

2.7 Evaluation of Aptamer–AuNP-Based LFA

The performance of the developed lateral flow assay was evaluated using varying concentrations of CA125 antigen. Standard antigen solutions were prepared over a concentration range of 0.1–1000 ng/mL.

For assay testing, a defined volume of the sample was applied to the sample pad, allowing it to migrate along the strip via capillary action. During migration, the target antigen interacted with the aptamer–AuNP conjugates to form complexes, which were subsequently captured at the test line through antibody–antigen interactions, resulting in the formation of a visible coloured band.

The intensity of the test line signal was monitored visually and, where applicable, quantified to evaluate assay sensitivity, detection range, and overall performance characteristics. The assay response was analyzed as a function of antigen concentration to assess its potential applicability for rapid and sensitive detection.

3. RESULTS

3.1 In Silico Screening and Lead Optimization of CA125-Specific Aptamers

A comprehensive *in-silico* screening pipeline was used to identify high-affinity aptamers targeting CA125. At first, a total of 4.1×10^6 random single-stranded DNA (ssDNA) sequences, each ranging from 30–45 nucleotides in length, were generated using the FaBox tool.

3.2 Primary Screening and Aptamer Probability Filtering

Primary screening of candidate sequences was performed using the aptamer prediction module of the PPAI webserver. The generated sequences were evaluated based on key aptamer-associated features, including nucleotide composition, GC content distribution, structural foldability, and machine learning-derived aptamer probability scores.

This filtering step significantly reduced the candidate pool to 1.793×10^6 sequences (~43%), representing structurally stable and compositionally favourable aptamer-like candidates.

3.3 Target-Specific Interaction Screening

The shortlisted sequences were further evaluated for their binding affinity toward CA125 using the aptamer–protein interaction module within the PPAI platform. Among these, approximately 1.3×10^6 sequences demonstrated measurable interaction with the target antigen.

Binding potential was quantified using the predicted pair score, which integrates sequence-derived physicochemical properties with protein interaction descriptors. From this subset, the top 80 candidates exhibiting pair scores greater than 0.58, indicative of moderate to strong binding affinity were shortlisted for further analysis (Table 1).

The pair score distribution among these candidates ranged from 0.58 to 0.61, with a median value of 0.584, suggesting a relatively narrow but high-affinity selection window.

3.4 Comparative Analysis with Literature-Reported Aptamers

To benchmark the performance of the predicted aptamers, a total of 83 previously reported aptamer sequences were also evaluated for binding affinity against CA125.

Notably, the majority of these sequences (73 aptamers) exhibited pair scores below 0.5, indicating comparatively weak binding affinity. Only 10 sequences demonstrated pair scores above 0.5, with the highest observed value being 0.56, which remained lower than the top predicted candidates from the present study.

This comparison highlights the improved binding potential of the newly designed aptamers over existing sequences.

3.5 Docking-Based Lead Optimization

Further refinement of candidate aptamers was performed through molecular docking analysis using pyDock and HDock tools. The top 10 aptamers from each docking platform were identified based on binding energy scores, and overlapping candidates across both methods were selected to ensure robustness of prediction.

To evaluate specificity, off-target binding analysis was conducted against 37 cancer-associated biomarkers with available 3D structures from the Protein Data Bank (PDB). This step ensured that selected aptamers exhibited preferential binding toward CA125 over other structurally related targets.

3.6 Identification of Lead Aptamer Candidates

This multi-step screening and optimization process resulted in the identification of the top-performing novel aptamer candidate, designated as P1, which demonstrated superior binding affinity, structural stability, and target specificity.

The sequences of the selected aptamers are as follows:

P1 (31 nt): GGGGTGTCATGTACACACTGGCATTCAAAT

P2 (42 nt): CGTTTATGTCTGGCAAATGCGCGATCGATTTTAAACGTACGCC

3.7 Docking Score Comparison

The comparative binding scores obtained from PPAI, HDOCK, and pyDock analyses are summarized below:

Table 1: Comparative binding scores of selected aptamers against CA125 obtained from PPAI prediction and molecular docking analyses (HDOCK and pyDock).

Aptamer	PPAI Score	HDOCK Score	pyDock Score
P1	0.61608	-278.7	-80.069
P2	0.60567	-306.5	-83.469
EX1	0.48512	-302.9	-69.826
EX2	0.56855	-277.5	-96.696

Among the candidates, P1 exhibited the highest PPAI score, indicating superior predicted binding affinity, while maintaining competitive docking scores across both platforms. Although P2 demonstrated slightly better docking energies in certain cases, its overall ranking across multiple parameters positioned P1 as the most balanced and promising candidate.

3.8 Selection of Lead Candidate for Experimental Validation

Based on integrated analysis of aptamer probability scores, docking energies, and off-target binding profiles, P1 was selected as the lead aptamer candidate for subsequent experimental validation and development of the lateral flow assay platform. The molecular docking interaction of P1 with CA125 is shown in figure 1.

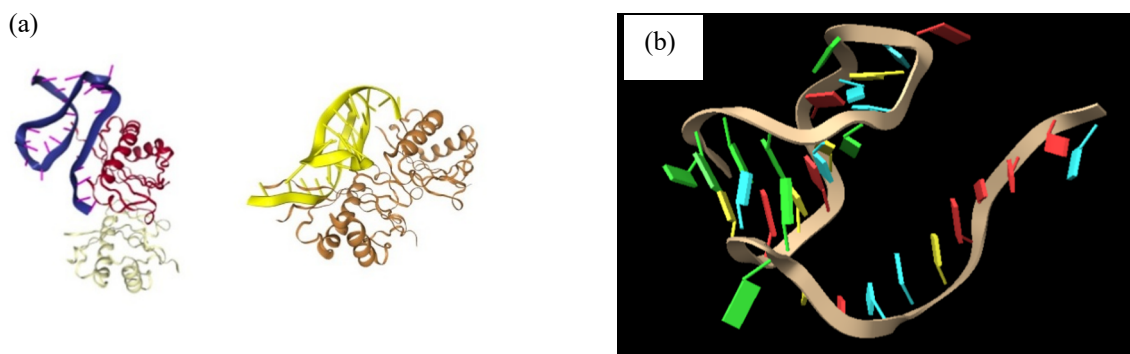


Figure 1: (a) Molecular docking interaction of the selected aptamer (P1) with CA125 showing binding orientation and interaction interface. (b) Predicted three-dimensional structure of the P1 aptamer highlighting its secondary structural features.

3.9 Characterization of Gold Nanoparticles

The synthesized gold nanoparticles were first characterized to confirm their suitability for lateral flow assay development. UV-visible spectroscopic analysis revealed a characteristic surface plasmon resonance (SPR) peak at approximately 521 nm (Figure 2(a), solid black colored curve), confirming the successful formation of colloidal gold nanoparticles.

The hydrodynamic radius of the synthesized nanoparticles, dispersed in a wine-red colloidal suspension (Figure 2(b)), was determined using dynamic light scattering (DLS) with a Malvern Zetasizer instrument. The size distribution exhibits a predominant intensity peak at approximately 37.8 nm, indicating the average particle diameter, along with a minor population of smaller-sized particles (see Figure 2(c)). The presence of a sharp and

well-defined peak indicates uniform particle size distribution and minimal aggregation, making the nanoparticles suitable for bioconjugation and signal generation in LFA applications.

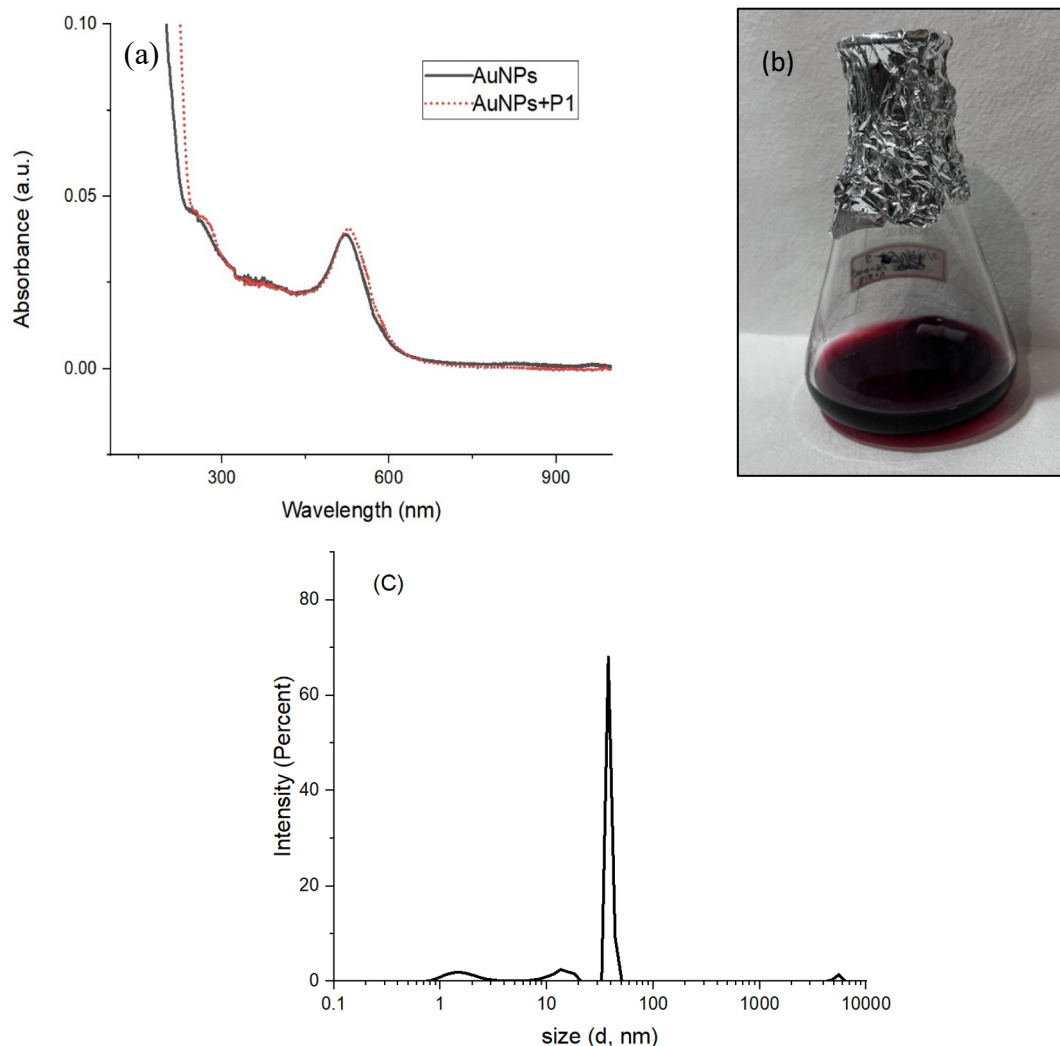


Figure 2: (a) UV-visible absorption spectrum of synthesized gold nanoparticles (AuNPs, black colored solid line) and P1-AuNPs conjugate (red colored dashed curve), (b) Photograph of the synthesized AuNP colloidal suspension exhibiting a wine-red color and (c) dynamic light scattering(DLS) spectra of the synthesized AuNPs colloidal suspension.

3.10 Formation of Aptamer–AuNP Conjugates

The AuNP particles were then incubated with P1 aptamer for one hour to prepare conjugates of P1-AuNPs. The 5'-biotinylated aptamer (P1) was successfully conjugated with AuNPs through non-covalent adsorption. Conjugation was confirmed by shift in the absorption maxima from 521 nm (AuNPs) to 527 nm(P1-AuNPs conjugate)(Figure 2(a) red colored dotted curve). The prepared conjugates exhibited excellent colloidal stability with no visible aggregation (absence of absorption peak or hump between 600-700 nm). The fact that the optical properties of nanoparticles stayed the same after conjugation showed that the functionalization method did not harm the nanoparticles' integrity.

The biotin part made it possible for streptavidin to interact with the control line, making sure it worked with the LFA format.

3.11 Fabrication of Lateral Flow Assay Strips

The LFA strips were meticulously designed with a multi-component structure that includes a sample pad, conjugate pad, nitrocellulose membrane, and absorbent pad. The anti-CA125 antibody was consistently immobilized at the test line, whereas streptavidin was applied at the control line.

The conjugate pad effectively retained the aptamer–AuNP conjugates after drying, and sufficient overlap between components enabled uninterrupted capillary flow down the strip.

3.12 Detection of CA125 Using LFA

We tested the analytical performance of the LFA we built using a constant concentration (10 ng/mL) of CA125 antigen. Application of the sample to the sample pad(SP) initiated capillary-driven flow, which helped the target antigen and the aptamer-AuNP conjugates present on conjugate pad(CP) interact with each other forming CA125-P1-AuNPs complex. Movement of the complex further towards the test line on nitrocellulose membrane resulted in antibody–antigen binding at the test line that was confirmed by red colored band on test line (see Figure 3).

At the same time, a strong signal appeared at the control (C) line confirmed binding of biotinylated aptamer-AuNPs via biotin-streptavidin complex formation. This also displayed that the sample fluid and conjugates were moving properly and the assay system was working. Excess of the sample fluid was absorbed by wicking pad (WP).

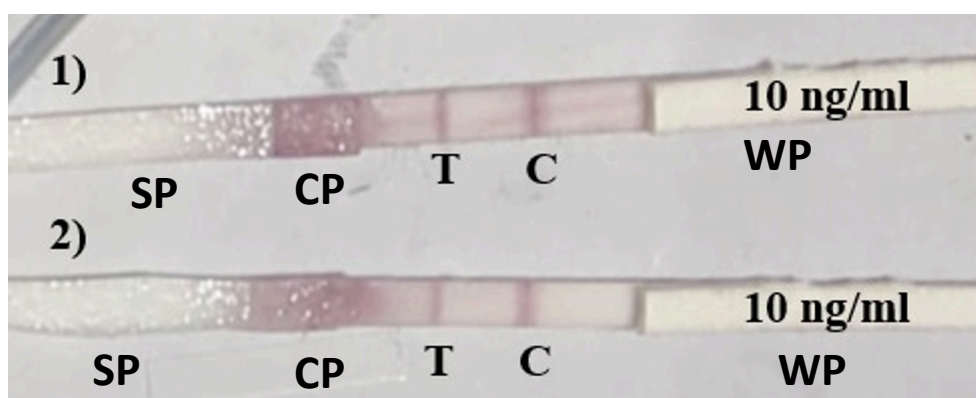


Figure 3: Detection of CA125 using the developed aptamer–AuNP-based lateral flow assay at 10 ng/mL. Visible bands at the test (T) and control (C) lines confirm successful target detection and proper assay functionality. Replicate strips demonstrate reproducibility of the assay.

The successful generation of a visible signal at the test line at 10 ng/mL demonstrates the capability of the developed aptamer–AuNP-based LFA to detect CA125 at clinically relevant concentrations. The clear distinction between test and control lines further supports the specificity and functionality of the designed aptamer.

Although the current study focuses on proof-of-concept validation, the results highlight the strong potential of this platform for rapid, point-of-care detection. Further studies involving quantitative analysis and broader concentration ranges will be necessary to establish sensitivity, limit of detection, and clinical applicability.

4. DISCUSSION

The present study demonstrates a comprehensive strategy for the development of a novel aptamer targeting CA125 through an integrated *in silico* and experimental approach, followed by its successful application in a lateral flow assay (LFA) platform. Nanomaterial based diagnostics in combination with computational aptamer design highlight a novel potential to obtain a rapid point-of-care detection. Aptamer-based detection of CA125 has been explored using various biosensing platforms, including optical, electrochemical, and surface plasmon resonance (SPR) systems.

By emphasizing how strong aptamers are as recognition elements, an example of a highly sensitive aptamer-based SPR biosensor showed great accuracy and recovery for detecting CA125 in serum, which shows how robust aptamers are as recognition elements [23], [24]. Similarly, luminescence-based aptasensors employing upconversion nanoparticles have achieved ultra-low detection limits (as low as 9.0×10^{-3} U/mL), although such systems often require sophisticated instrumentation and are susceptible to signal interference [25].

Unlike these other methods, the current study focuses on a lateral flow format, which is more easier to use, portable and responds quickly. In addition to this, it is well known that paper-based biosensors, such as LFAs, are great for point-of-care diagnostics since they are cheap and easy to use. There are just a few studies that have talked about

using aptamer-based LFA systems to find CA125, one of which showed P. Tripathi et al. creating a competitive lateral flow assay based on an aptamer-gold nanozyme that can find CA125 in human serum with a detection limit of about 5.21 U/mL [10]. Their solution used nanoparticles that act like enzymes to boost signal output, and it worked well with normal ELISA procedures. Compared to this study, the present work introduces a novel aspect at the level of aptamer design, where candidates were generated and optimized entirely through a bioinformatics-driven pipeline rather than relying solely on experimentally derived sequences (e.g., SELEX).

This computational approach made it possible to rapidly evaluate millions of sequences and produced aptamers with a higher anticipated binding affinity than most sequences described in the literature. Also, although earlier LFA investigations frequently use antibody–antigen or competitive assay formats, the current approach shows a hybrid aptamer–antibody setup, with the aptamer as the recognition element and antibodies as the capture element. This architecture makes the system more flexible and may make the assay more stable than systems that are based only on antibodies.

SELEX and other traditional approaches for finding aptamers are time consuming and costly. Computational methods have become strong options for quickly screening and improving aptamers in the last few years. The current study illustrates that *in silico* techniques can successfully identify high-affinity aptamers with enhanced binding scores relative to numerous previously documented sequences. The integration of machine learning-based prediction (PPAI), docking analysis (HDOCK and pyDock), and off-target screening provides a multi-layer validation strategy, improving confidence in the selected candidates. This approach aligns with recent trends emphasizing the use of computational tools to accelerate biosensor development [26].

The successful conjugation of aptamers with gold nanoparticles further reinforces the applicability of nanomaterials in biosensing. Gold nanoparticles are widely used in LFA systems due to their strong optical properties and ease of functionalization. Previous studies have demonstrated that aptamer–nanomaterial conjugates enhance detection performance and enable versatile sensing platforms [26].

Although UV–visible spectroscopy and dynamic light scattering technique confirmed the formation of gold nanoparticles and its hydrodynamic radius was evaluated, but size estimation using transmission electron microscopy and stability of nanoparticles using zeta potential was not performed in this study. Future work will include comprehensive physicochemical characterization to better correlate nanoparticle size and stability with assay performance. In the present work, the retention of a sharp SPR peak and stable conjugate formation confirms that the designed aptamer is compatible with nanoparticle-based detection systems, which is critical for real-world applications. The developed aptamer–AuNP-based LFA successfully detected CA125 at 10 ng/mL, producing clear and reproducible visual signals. While the current study focuses on proof-of-concept validation, the observed signal clarity and reproducibility indicate that the system has strong potential for further optimization.

Compared to previously reported systems, which often involve signal amplification strategies or complex detection mechanisms, the present assay demonstrates that simple visual detection is achievable using computationally designed aptamers, highlighting its practical applicability.

Despite these promising results, the current study is limited to validation at a single antigen concentration. Previous studies have demonstrated the importance of evaluating parameters such as limit of detection (LOD), sensitivity, and specificity across a wide dynamic range for clinical applicability [10]. Formal determination of the limit of detection (LOD) is not attempted in this present study, as its primary objective was to demonstrate proof-of-concept validation of the developed platform. Future investigations will evaluate assay performance over an extended concentration range to establish sensitivity, LOD, and dynamic range.

5. CONCLUSION

This research successfully developed an innovative aptamer targeting CA125 through a comprehensive *in silico* screening process, which was later validated via experimental application in a lateral flow assay (LFA) platform and this computational approach facilitated the rapid screening of an extensive library of sequences, resulting in the identification of high-affinity aptamer candidates with superior predicted binding properties compared to previously published sequences.

Among the shortlisted candidates, the aptamer P1 demonstrated optimal binding affinity, structural stability, and target specificity, and was selected for further experimental validation. The successful synthesis and characterization of gold nanoparticles, along with their stable conjugation with the aptamer, enabled effective signal generation within the LFA format.

The developed aptamer–AuNP-based LFA demonstrated clear and reproducible detection of CA125 at a concentration of 10 ng/mL, confirming the feasibility of the proposed platform for rapid and visual detection. The incorporation of a streptavidin-based control line further ensured assay reliability and functional validation.

This study underscores the possibility of combining bioinformatics-driven aptamer design with nanomaterial-based lateral flow systems to provide quick, cost-effective, and point-of-care diagnostic tools. Although the present study provides a proof-of-concept, subsequent research concentrating on quantitative performance assessment, clinical sample validation, and assay refinement will be crucial for the translation of this platform into practical diagnostic applications.

References

- [1] M. K. Hong and D. C. Ding, “Early Diagnosis of Ovarian Cancer: A Comprehensive Review of the Advances, Challenges, and Future Directions,” *Diagnostics* **2025**, Vol. 15, vol. 15, no. 4, Feb. 2025, doi: 10.3390/DIAGNOSTICS15040406.
- [2] G. Funston, W. Hamilton, G. Abel, E. J. Crosbie, B. Rous, and F. M. Walter, “The diagnostic performance of CA125 for the detection of ovarian and non-ovarian cancer in primary care: A population-based cohort study,” *PLoS Med.*, vol. 17, no. 10, Oct. 2020, doi: 10.1371/JOURNAL.PMED.1003295.
- [3] S. Bayoumy *et al.*, “Glycovariant-based lateral flow immunoassay to detect ovarian cancer-associated serum CA125,” *Communications Biology* **2020** 3:1, vol. 3, no. 1, pp. 460-, Aug. 2020, doi: 10.1038/s42003-020-01191-x.
- [4] B. Asci Erkocyigit, O. Ozufuklar, A. Yardim, E. Guler Celik, and S. Timur, “Biomarker Detection in Early Diagnosis of Cancer: Recent Achievements in Point-of-Care Devices Based on Paper Microfluidics,” *Biosensors* **2023**, Vol. 13, vol. 13, no. 3, Mar. 2023, doi: 10.3390/BIOS13030387.
- [5] P. S. Filippou and P. Dey, “Proteomic Biomarkers and Diagnostic Tools in Ovarian Cancer: Understanding Their Clinical Value and Limitations,” *J. Proteome Res.*, vol. 24, no. 7, pp. 3137–3153, Jul. 2025, doi: 10.1021/ACS.JPROTEOME.5C00088.
- [6] A. Abdelwahed *et al.*, “A Rational Optimization Approach for the Development of a Multiplexed Lateral Flow Immunoassay: Detection of Nonepithelial Ovarian Cancer Markers in Human Serum,” *Advanced Science*, p. e23192, 2026, doi: 10.1002/ADVS.202523192
- [7] S. Kakkar *et al.*, “Lateral flow assays: Progress and evolution of recent trends in point-of-care applications,” *Mater. Today Bio*, vol. 28, p. 101188, Oct. 2024, doi: 10.1016/J.MTBIO.2024.101188.
- [8] D. M. Kinyua, D. M. Memeu, C. N. Mugo Mwenda, B. Della Ventura, and R. Velotta, “Advancements and Applications of Lateral Flow Assays (LFAs): A Comprehensive Review,” *Sensors* **2025**, Vol. 25, vol. 25, no. 17, Sep. 2025, doi: 10.3390/S25175414.
- [9] J. Pedreira-Rincón *et al.*, “A comprehensive review of competitive lateral flow assays over the past decade,” *Lab Chip*, vol. 25, no. 11, pp. 2578–2608, May 2025, doi: 10.1039/D4LC01075B.
- [10] P. Tripathi, A. Kumar, M. Sachan, S. Gupta, and S. Nara, “Aptamer-gold nanozyme based competitive lateral flow assay for rapid detection of CA125 in human serum,” *Biosens. Bioelectron.*, vol. 165, Oct. 2020, doi: 10.1016/J.BIOS.2020.112368.

- [11] M. Majdinasab, M. Badea, and J. L. Marty, "Aptamer-Based Lateral Flow Assays: Current Trends in Clinical Diagnostic Rapid Tests," *Pharmaceuticals* 2022, Vol. 15, vol. 15, no. 1, Jan. 2022, doi: 10.3390/PH15010090.
- [12] M. Ekman, T. Salminen, K. Raiko, T. Soukka, K. Gidwani, and I. Martiskainen, "Spectrally separated dual-label upconversion luminescence lateral flow assay for cancer-specific STn-glycosylation in CA125 and CA15-3," *Anal. Bioanal. Chem.*, vol. 416, no. 13, pp. 3251–3260, May 2024, doi: 10.1007/S00216-024-05275-Z.
- [13] D. J. Scoville, T. K. B. Uhm, J. A. Shallcross, and R. J. Whelan, "Selection of DNA Aptamers for Ovarian Cancer Biomarker CA125 Using One-Pot SELEX and High-Throughput Sequencing," *J. Nucleic Acids*, vol. 2017, 2017, doi: 10.1155/2017/9879135.
- [14] P. Tripathi, M. Sachan, and S. Nara, "Novel ssDNA Ligand Against Ovarian Cancer Biomarker CA125 With Promising Diagnostic Potential," *Front. Chem.*, vol. 8, p. 531203, May 2020, doi: 10.3389/FCHEM.2020.00400.
- [15] D. J. Chinchilla-Cárdenas *et al.*, "Current developments of SELEX technologies and prospects in the aptamer selection with clinical applications," *Journal of Genetic Engineering and Biotechnology*, vol. 22, no. 3, Sep. 2024, doi: 10.1016/j.jgeb.2024.100400.
- [16] J. X. Hu and S. N. Ding, "In Situ Synthesis of Highly Fluorescent, Phosphorus-Doping Carbon-Dot-Functionalized, Dendritic Silica Nanoparticles Applied for Multi-Component Lateral Flow Immunoassay," *Sensors*, vol. 24, no. 1, p. 19, Jan. 2024, doi: 10.3390/S24010019/S1.
- [17] E. Lamprou, P. M. Kalligosfyri, and D. P. Kalogianni, "Beyond Traditional Lateral Flow Assays: Enhancing Performance Through Multianalytical Strategies," *Biosensors* 2025, Vol. 15, vol. 15, no. 2, Jan. 2025, doi: 10.3390/BIOS15020068.
- [18] P. Villesen, "FaBox: an online toolbox for fasta sequences," *Mol. Ecol. Notes*, vol. 7, no. 6, pp. 965–968, Nov. 2007, doi: 10.1111/J.1471-8286.2007.01821.X.
- [19] J. Li, X. Ma, X. Li, and J. Gu, "PPAI: a web server for predicting protein-aptamer interactions," *BMC Bioinformatics* 2020 21:1, vol. 21, no. 1, pp. 236–, Jun. 2020, doi: 10.1186/S12859-020-03574-7.
- [20] Y. Yan, D. Zhang, P. Zhou, B. Li, and S. Y. Huang, "HDOCK: a web server for protein–protein and protein–DNA/RNA docking based on a hybrid strategy," *Nucleic Acids Res.*, vol. 45, no. W1, pp. W365–W373, Jul. 2017, doi: 10.1093/NAR/GKX407.
- [21] T. M. K. Cheng, T. L. Blundell, and J. Fernandez-Recio, "PyDock: Electrostatics and desolvation for effective scoring of rigid-body protein-protein docking," *Proteins: Structure, Function and Genetics*, vol. 68, no. 2, pp. 503–515, Aug. 2007, doi: 10.1002/PROT.21419.
- [22] J. Kimling, M. Maier, B. Okenve, V. Kotaidis, H. Ballot, and A. Plech, "Turkevich Method for Gold Nanoparticle Synthesis Revisited," *Journal of Physical Chemistry B*, vol. 110, no. 32, pp. 15700–15707, Aug. 2006, doi: 10.1021/JP061667W.
- [23] S. Valizadeh Shahbazlou, S. Vandghanooni, B. Dabirmanesh, M. Eskandani, and S. Hasannia, "Biotinylated aptamer-based SPR biosensor for detection of CA125 antigen," *Microchemical Journal*, vol. 194, p. 109276, Nov. 2023, doi: 10.1016/J.MICROC.2023.109276.
- [24] V. R. Kumar, N. C. Kampan, N. H. Abd Aziz, C. K. Teik, M. N. Shafiee, and P. S. Menon, "Recent Advances in Surface Plasmon Resonance (SPR) Technology for Detecting Ovarian Cancer Biomarkers," *Cancers* 2023, Vol. 15, vol. 15, no. 23, Nov. 2023, doi: 10.3390/CANCERS15235607.
- [25] X. Zhang *et al.*, "An aptamer biosensor for CA125 quantification in human serum based on upconversion luminescence resonance energy transfer," *Microchemical Journal*, vol. 161, Feb. 2021, doi: 10.1016/J.MICROC.2020.105761.
- [26] A. Mohammadinejad *et al.*, "Aptamer-Based Targeting of Cancer: A Powerful Tool for Diagnostic and Therapeutic Aims," *Biosensors* 2024, Vol. 14, vol. 14, no. 2, Jan. 2024, doi: 10.3390/BIOS14020078.